Better molecular preservation of organic matter in an oxic than in a sulphidic depositional environment: evidence from of *Thalassiphora pelagica* (Dinoflagellata, Eocene) cysts.

Gerard J. M. Versteegh[1,2], Alexander J. P. Houben[3,4], Karin A.F. Zonneveld[2]

5 [1]Heisenberg Group Marine Kerogen, Marum Research Faculty, Universität Bremen, Bremen, D-28359, Germany.
[2] Micropaleontology Group, Division Marine Palynology, Marum Research Faculty, Universität Bremen, Bremen, D-28359, Germany.
[3]Geological Survey of the Netherlands, TNO, Utrecht, 3548 CB, The Netherlands.
[4]Marine Palynology and Palaeoceanograhy, Faculty of Geosciences, Utrecht University, Budapestlaan 4, 3584 CD Utrecht,
10 The Netherlands.

Correspondence to: Gerard J. M. Versteegh (versteeg@uni-bremen.de)

Abstract. Anoxic sediments as compared to oxic settings encompass a much higher proportion of relatively labile and thus
15 more reactive organic matter, naturally giving rise to condensation reactions (such as vulcanisation) transforming the original biomolecules into geomolecules. For the oxic environment where the labile, reactive, component is rapidly removed, such transformation and condensation is much less likely so that one would expect a structurally much better preservation of the more refractory initial biomolecules. To test this hypothesis, initially identical biomolecules need to be compared between different preservational environments. Here, we use the species specific morphology of organic microfossils to assure a
20 single initial biosynthetic product (the cysts of the fossil dinoflagellate species *Thalassiphora pelagica*) for comparison. We assess the macromolecular structures of cysts from the Eocene (~40 Ma) sulphidic Rhine Graben and the oxic Kerguelen Plateau and compare them with each other and the structures of recent cysts. While between the sites the *T. pelagica* cysts are morphologically identical, pyrolysis gas chromatography mass spectroscopy and micro Fourier transform infra red analyses show that their macromolecular characteristics are strongly different. The cysts deposited in the sulphidic Rhine
25 Graben show a strong contribution of long-chain aliphatic moieties and organic sulphur, absent in the material deposited on the oxic Kerguelen Plateau. Comparison with recent cyst walls suggests a much better molecular preservation for the oxic depositional environment, confirming our initial hypothesis. This leads to the conclusion that the best preservation of molecular structure is not necessarily where most organic matter gets preserved, which, in turn, is important for understanding the nature and fate of sedimentary organic matter.

30 **1 Introduction**

Kerogen, the insoluble sedimentary organic matter (OM) is by far the largest organic matter pool on Earth (Durand, 1980). It plays an important role in the biogeochemical cycles of carbon and related elements, fossil fuel formation and is a source of

information on the history of life and environments. Despite considerable advances in elucidating the nature of kerogen over the last decades, many aspects of the formation, structure and modification of especially marine kerogen are still far from

35 understood (Vandenbroucke, and Largeau, 2007; de Leeuw and Largeau, 1993). This is particularly true for marine kerogen where the heterogeneity and the small size of the kerogen particles are complicating factors in the effort to understand of kerogen formation and modification.

Analysis of organic (micro)fossils enables a direct link between the biological source (often at species level) and fossil structure, for different environments and time-slices. As such it allows for separating the contributions of biosynthesis and

40 post-mortem modification on the final kerogen structure.

Chemical analysis of organic (micro)fossils has shown that despite excellent morphological preservation, chemical preservation may be poor (e.g. Stankiewicz et al., 2000; Stankiewicz et al., 1998; Gupta et al., 2007; de Leeuw et al., 2006). In oxic settings, organic matter degradation is mostly severe and highly selective but nevertheless processes like photodegradation and oxidative polymerization may lead to condensation of the OM, already early in the fossilization

45 process which reduces OM degradability, creates macromolecules from lipids and transforms biomacromolecules into geomacromolecules (e.g. Versteegh et al., 2004; Harvey et al., 1983; Rontani, 2008; Gatellier et al., 1993). In anoxic settings OM degradation is much less complete, leading to the formation of organic-rich sediments (e.g. Bianchi et al., 2016). Here, condensation of organic matter may occur through sulphurisation, especially in the absence of sufficient electron donors like Fe, scavenging the (poly)sulfides and preventing them to crosslink the organic matter (Kohnen et al., 1989; Nissenbaum, and

50 Kaplan, 1972).

Most of these insights have been obtained by analyzing different taxa from unique sedimentary environments. Which makes it hard to obtain insight in the relation between the species specific properties of its organic product and the subsequent post-mortem modification. For such a better separation of initial organic matter and post-mortem modification ideally one would analyse the same biomacromolecule from different environmental settings.

55 Here we elucidate the influence of differing sedimentary environments on the chemical preservation of same species, fossil dinoflagellate cysts of *Thalassiphora pelagica*.

The molecular structure of the walls of extant organic dinoflagellate cysts, where known, may vary considerably between species (e.g. Mertens et al., 2016; Bogus et al., 2014; Gurdebeke et al., 2018). They all seem to consist of a carbohydrate-backbone but with various contributions of proteinaceous material that appears to be species specific (Versteegh et al., 2012;

60 Bogus et al., 2014). Basically the same variability has been reported from fossil material where the molecular structure could even be used to distinguish between closely related *Apectodinium* species (Bogus et al., 2012). However, it became apparent that in some cases post-mortem modification may considerably change the molecular structure of the cyst wall. For instance, contributions of long-chain aliphatic moieties have been reported for *Chiropteridium* spp. (de Leeuw et al., 2006) and *T. pelagica* cysts from the Oligocene Rhine Graben (Versteegh et al., 2007). These modifications may be so pronounced that

65 the original signature is largely lost (de Leeuw et al., 2006; Versteegh et al., 2007). However, the extent to which

environment transforms the initial biomacromolecule to its geomacromolecular derivate is still to a large extent terra incognita.

Here we concentrate on the impact of oxic versus anoxic sedimentary environments on the macromolecular structure of *T. pelagica* cysts, a microfossil known to be resistant to aerobic degradation. The molecular structure of cysts of this species

70   that were deposited under anaerobic sulfate reducing conditions has already been discussed (2007). Characterization of the molecular composition of the cyst walls with FTIR micro-spectroscopy, py-GC-MS and thermally assisted hydrolysis and methylation (THM)-GC-MS showed that the cyst wall macromolecule of these cysts is relatively condensed which is in line with the condensation of an initially carbohydrate-based wall biomacromolecule. Nevertheless, an average chain length of ~ 12 carbon atoms was recorded which was explained by post-mortem addition of carboxylic acids by early sulphurisation of

75   the cysts in the anoxic to suboxic setting of the depositional environment. Here we compare the results of the study on anoxically deposited and sulphurised *T. pelagica* cysts to new analysis of cysts of the same species that have been deposited in an oxic depositional environment. This allows us to determine the diagenetic effects of aerobic versus anaerobic sulfate reducing environments on the molecular structure of organic microfossils.

2 Material and Methods

80   The *T. pelagica* cysts from the oxic depositional environment (Kerguelen Plateau) have been collected during IODP Leg 120 Site 748B (58°26.45'S, 78°58.89'E) and have been isolated from sample 18H 17W 55-57 cm. The sample was crushed and minerals were removed using HCl (36%) and HF (40%) at room temperature. The sample was washed and the > 20 μm fraction was mounted to enable palynofacies analysis by light microscope.

The processing of *T. pelagica* cysts from the sulfate reducing environment (Rhine Graben) has been thoroughly discussed in

85   (Versteegh et al., 2007). This latter material was deposited in a marine setting with photic-zone anoxia. The samples were processed subsequently with 20 % HCl to remove carbonates. The samples were washed through sieves and from the125-315 μm fraction clean cysts were picked for further analysis with FTIR micro-spectroscopy, py-GC-MS and THM-GC-MS.

2.1 FTIR Analysis

The cysts from the Kerguelen Plateau were analysed by micro-FTIR after cleaning the cysts with distilled water and

90   methanol. Only specimens were measured that were visually clean. Measurements were made with a BRUKER Invenio-S spectrometer coupled to a Hyperion 1000 IR microscope equipped with a KBr beamsplitter and liquid N2-cooled MCT detector. Two hundred and fifty-six scans were obtained at 4 cm^{-1} resolution using a germanium ATR crystal of 100 μm diameter. The spectra were corrected for atmospheric CO2 and baseline corrected using a concave rubberband correction 64 baseline points and 10 iterations. To make the spectra comparable to those of the *T. pelagica* specimens of the Rhine Graben

95   material, the ATR spectra have been transformed such that the position and intensity of the absorption bands are similar to those of a spectrum acquired in transmission mode by using the advanced ATR correction algorithm (Nunn, and Nishikida,

2008). Assignments of characteristic IR group frequencies follow Colthup, Daly, and Wiberly (1990) and published literature.

100 For FTIR micro-spectroscopic analyses of *T. pelagica* specimens of the Rhine Graben material see (Versteegh et al., 2007). For baseline subtraction, calculation of first and second derivatives and fitting of Gaussian curves the software package Fytik 1.2.1 has been used (Wojdyr, 2010).

2.2 Pyrolysis and thermally assisted hydrolysis and methylation gas chromatography-mass spectrometry

The cysts from the Kerguelen Plateau were solvent extracted and transferred to a quartz tube (CDS 10A1-3015) for
105 pyrolysis. For thermally assisted hydrolysis and methylation (THM) in the presence of TMAH about 0.2 ml of 10% aqueous TMAH were added and the quartz tube oven dried for 1 h at 60 °C. The sample was inserted in a CDS 5200 pyrolysis unit and kept for 5 min at 700 °C. The pyrolysate and thermochemolysate were transferred to a gas chromatograph Agilent 7890A series using a 300 °C interface and transfer-line temperature. Splitless mode, delay time 6 min. GC column HP5MS, 30 m length, 0.25 mm diameter, 0.25 μm film thickness. GC conditions: 3 min iso-therm at 40 °C, 15 °C/min to 130 °C, 8
110 °C/min to 250 °C, 20 °C/min to 320 °C and 5 min isotherm. Interface temperature 280 °C GC to MS. For mass spectrometry an Agilent 5975C MSD was used in full scan mode (mass range m/z 50-500, 3.25 scans/s, 70 eV). Compound identification was performed using the NIST spectral library and retention times.

For Pyrolysis and thermochemolysis gas chromatography-mass spectrometry of the cysts from the Rhine Graben (see Versteegh et al., 2007).

115 ## 3 Results

3.1 Palynofacies analysis

The assemblage consists of a nearly monotypical assemblage *T. pelagica* cysts with occasional *Phthanoperidinium* and indeterminable organic debris (Fig 1). The residue left after additional purification with a sieve with 50 μm pore-size consisted of *T. pelagica* cysts only.

120 ### 3.2 FTIR micro-spectroscopy

Three specimens of *T. pelagica* were analysed, each at least twice. The FTIR spectra are closely similar and therefore, only the average spectrum is shown (Fig. 2). The spectrum can be divided into six absorption bands (A—F). Band A shows a low broad absorption centred at 3400 cm^{-1} and a minor absorption at 3036 cm^{-1}. Band B, (3000 cm^{-1}—2700 cm^{-1}) is the least intense. It shows absorption maxima at 2929 and 2854 cm^{-1}. Band C (1800 and 1500 cm^{-1}) absorbs stronger than A and B.
125 Absorption maxima are at 1707 and 1610 cm^{-1}. Absorption in band D (1500—1300 cm^{-1}) has a maximum at 1411 cm^{-1} and an intensity similar to band C. Band E (1300—1150 cm^{-1}) shows a continuation of band D with respect to the decrease in

absorption. Band F (1150—900 cm^{-1}) has the strongest absorption of the entire spectrum at 1047 cm^{-1}. Finally, band G (900—700 cm^{-1}) contains narrow and relatively minor absorptions of which the one at 857 cm^{-1} is the most prominent. The second derivative reveals the locations of narrower absorption maxima absorptions in shoulders in much more detail (Fig. 3)

130 whereby three Gaussian/Lorentzian bands can be fitted in the aliphatic C-H$_x$ stretching region from 3000—2700 cm^{-1} (Fig 4).

3.3 Pyrolysis–GC-MS

The pyrolysate (Fig.5; Table 1) contains both aliphatic and aromatic moieties. There is a considerable number of oxygen containing saturated and unsaturated non-aromatic moieties with 5-membered and 6-membered rings and up to three

135 additional carbon atoms amongst which are furans, cyclopente/anones, phenols, benzofurans, indanones and naphthalenones and naphthalenols. Furthermore, there are several series of aromatic moieties. Phenol (m/z 94) and methylated phenols (m/z 94 + 14 * n) have been detected up to $n = 4$. Benzene (m/z 78) and alkyl benzenes (m/z 78 + 14 * n) have been detected up to $n = 9$. Compounds with more than three carbon atoms attached to naphthalene and indene were not detected. Linear carbon chains play only a minor role and their distribution becomes only apparent from mass chromatograms of their characteristic

140 ions. n-Alkanes and n-alkenes (m/z 83 and 85) show alkane/alkene pairs for C$_7$ - C$_9$ and a series of only n-alkanes for C$_{14}$ - C$_{21}$. The mass chromatogram m/z 58 reveals a series of n-alkan-2-one / n-alken-2-one pairs from C$_6$ - C$_{12}$ and m/z 60 shows C$_3$ - C$_{10}$ alkanoic acids.

The mass distribution in the first 28 min of the chromatogram (Fig. 6) shows that the masses representing aromatic moieties (such as m/z 91, 105, 115, 117, 119, 128, 129) clearly emerge above their neighbour masses (m/z ± 5). The masses

145 representing saturated aliphatic moieties (m/z 57, 71, 85) do not emerge above background as is the case for alkenes > C$_5$ (m/z 83, 97).

3.3 THM–GC-MS

THM-GC-MS (Fig.7; Table 2) clearly shows methyl esters of C$_3$—C$_9$ and C$_{14}$—C$_{16}$ n-alkanoic acids (C$_{17}$ and C$_{18}$ could not be detected) and C$_4$—C$_9$ α,ω dicarboxylic-dimethylesters the latter with a strong preference for the butanedioic moiety. Few

150 oxygen containing aromatic compounds are present. The most prominent are mono- to tri-methoxy benzenes and mono-and dimethoxy benzoic-acid methylesters. Traces of alkane/alkene doublets (using m/z 83/85) are absent.

4 Discussion

4.1 FTIR Spectroscopy

4.1.1 The FTIR spectra of the *T. pelagica* cysts from the oxic depositional environment (Kerguelen Plateau; Figs. 2-4)

155 The absorption of band A, centred at 3400 cm^{-1} is assigned to alcoholic OH, phenolic OH, and/or carboxylic OH.

The strong, narrow aliphatic absorptions of band B, centred at 2934 and 2858 cm^{-1} are assigned to antisymmetric stretching vibrations from CH$_2$ and symmetric stretching vibrations from CH$_2$ methylene groups, respectively. Further deconvolution shows that a third Gaussian/Lorentzian band at 2892 cm^{-1} is required to model this part of the spectrum (Fig 4). This third band is attributed to CH stretch. There is a marked absence of evidence for absorptions by CH$_3$. In algal walls

160   such a low contribution of methyl groups is typically associated with the presence of long aliphatic chains in the wall macromolecule, such as the algaenan of e.g. *Chlorella emersonii* (Fig 2.). However, the corresponding absorption of CH$_2$ in long carbon chains near 723 cm^{-1} (see also McMurry, and Thornton, 1952) is also absent from our spectra leading to the conclusion that the *T. pelagica* wall macromolecule consists primarily of short carbon chains without free methyl groups.

For band C the absorption centred at 1708 cm^{-1} as well as the shoulder 1768 cm^{-1} we assign to the vibration of

165   carbonyl C=O. Hereby, the absorption at 1708 cm^{-1} may represent conjugated aliphatic ketones or hydrogen bonding in carboxylic acid dimers (Colthup et al., 1990) the corresponding -enol tautomers may provide a second explanation for the moderate absorption centred at 1612 cm^{-1}.

For band D, the absorption at 1411 cm^{-1} may be attributed to deformation of CH$_2$ next to carbonyls. Alternatively the absorption at 1411 cm^{-1} may arise from olefin CH rocking. Absorptions at 1463 cm^{-1} we relate to scissors deformation of

170   CH$_2$. There is no clear symmetric umbrella deformation of C-CH$_3$ at 1375 cm^{-1} of hydrocarbons, which agrees with the absence of evidence for methyl groups in band B. The weakly defined absorptions between 1305 and 1203 cm^{-1} (Band E) can be related to C-O carboxylic acids.

For bands F, the absorptions at 1112, 1047, and 986 cm^{-1} are assigned to C-O e.g. as C-O-C and C-O-H of carbohydrates.

175   For band G the minor absorption at 728 cm^{-1} is attributable to CH$_2$ rock, its low intensity agrees with only a minor contribution of predominantly short carbon chains < 4 CH$_2$ sequences (McMurry, and Thornton, 1952).

As such the spectrum indicates a relatively short-chain polymer, rich in C-O, and -OH and a considerable number of =O. There is possibly some aliphatic C=C.

4.1.2 Comparison with FTIR spectra of *T. pelagica* cysts from the oxic environment (Kerguelen Plateau) and of other
180   **dinoflagellate species (Fig. 2)**

T. pelagica cysts are transparent gonyaulacoid dinoflagellate cysts. Infrared analysis of fresh cysts shows that their infra-red spectra cluster in two groups (Bogus et al., 2014; Ellegaard et al., 2013). (1) Transparent cysts with a cellulose-like cyst wall such as *Lingulodinium polyedrum* (Versteegh et al., 2012), and (2) Brown cysts with a chitin-like cyst wall such as *Polykrikos kofoidii* (Bogus et al., 2014). The former are produced by dinoflagellates with a predominantly phototrophic life

185   style, the latter by species with a predominantly heterotrophic life style. The *Thalassiphora* cysts belong to the first group. Within these groups there is considerable structural variation between the different species (Versteegh et al., 2012; Mertens et al., 2016; Mertens et al., 2015; Mertens et al., 2015; Bogus et al., 2014; Gurdebeke et al., 2018; Luo et al., 2018).

The spectra of cyst walls of *T. pelagica* from the Kerguelen Plateau and recent, culture derived *L. polyedrum* (Versteegh et al., 2012) share the characteristic strong absorption of band F (C-O). Band A (CH_x) is similar. Band C (C=O) is clearly

190 stronger for the *T. pelagica* cysts suggesting a higher carboxylic contribution. Nevertheless, the *T. pelagica* cysts differ from the fresh dinosporin of *Lingulodinium* in having relatively stronger absorptions by CH_2, CH_3 and C=O are weaker absorption by C-O. Infra-red analysis of extant cysts of other members of this group of Gonyaulacoid dinoflagellate cysts show structural differences between the species (Bogus et al., 2014; Gurdebeke et al., 2018). Hence, the question arises to which part of the differences recorded between the spectra of these *T. pelagica* with other Gonyaulacoid taxa arises from

195 differences in cyst biosynthesis and what part arises from post-mortem modification. The spectra of the recent Gonyaulacoid cysts show a consistent pattern in their order of absorption strength for bands D and E with band F being strongest and band E weakest. This pattern is also seen for the cysts from the Kerguelen Plateau. However, for band C this is more complicated. Analysis of recent cysts by Bogus et al. (2014) shows for all members of the Gonyaulacaceae (*Lingulodinium, Spiniferites, Impagidinium, Protoceratium*) a band C with weaker absorption than bands D and E). In Gurdebeke et al. (2018), all

200 members of the gonyaulacacean *Spiniferites* (except *S. pachydermus* which spectrum was taken from Bogus et al., 2014) show a strong absorption near 1600 cm^{-1} in band C that exceeds the absorptions in band D. This we also see for *T. pelagica* which, considering the variability of this band in recent cysts, we consider intrinsic feature of the biopolymer. In band C recent gonyaulacacean cysts also show a shoulder near 1705 cm^{-1}, which is always of much smaller amplitude than the absorption 1590 cm-1. This is clearly different for *T. pelagica* for which this is the most pronounced absorption in band C

205 and which for its absence in recent cysts we attribute to diagenesis. It represents absorptions by C=O of the kind typically also present in e.g. algaenan of *C. emersonii* (Fig. 2). This is a typical and common feature of post—mortem modification, a phenomenon that easily occurs, even already in the water column (Blom, 1936; Harvey et al., 1983; Versteegh et al., 2004; Stankiewicz et al., 2000).

4.1.3 Comparison of the micro-FTIR spectra of *T. pelagica* cysts from the oxic environment (Kerguelen Plateau) and
210 the anoxic Rhine Graben

The cysts from the Rhine Graben and the Kerguelen Plateau represent the same species *T. pelagica*. Therefore, we may assume identical or at least closely similar chemical structures prior to diagenesis so that all spectral differences between them logically reflect differences in chemical preservation. These differences show a further alteration in the same direction as the differences between *T. pelagica* cysts of the Kerguelen Plateau and the unaltered cysts represented by *L. polyedrum*.

215 This is demonstrated by a much stronger absorption of band B (CH_x), and a weaker absorption of band D and almost no absorption in band E (C-O). In that respect, the spectrum of the Rhine Graben specimens is much more similar to that of the algaenan walls of green algae such as *C. emersonii* (Allard, and Templier, 2001) or *Tetraedron minimum* (Blokker et al., 1998; Goth et al., 1988). Without the absorption at 718 cm^{-1} and thus lacking the long carbon chains of algaenan).

4.2 py-GC-MS and THM-GC-MS

220 Results of the GC-MS analyses support the above suggested depositional environment related alterations in molecular structure. Pyrolysis of macromolecules consisting of long alkyl chains, such as algaenans or polyethylene, typically produces a series of alkane/alkene doublets (Fig. 5). The presence of such n-alkane/alkene doublets up to C_9 (and similarly C_7—C_{11} methyl-alkanone/alkenone doublets) in the cysts from the Kerguelen Plateau suggests that these have been derived from the cyst macromolecule. The absence of alkane/alkene doublets from C_{10} in these cysts suggests that the aliphatic chains were

225 relatively short which agrees with the infrared spectrum. The absence of > C_{10} n-alkanoic acids supports this further. The presence of n-alkanes only for C_{14}—C_{21} and their absence for C_{10}—C_{13} suggests that these longer compounds were not covalently bound to the cyst macromolecule and they may have been absorbed by the cyst wall and failed to be removed upon extraction.

For the Kerguelen Plateau cysts we find a similar gap in distribution in the n-alkanoic methyl-esters released upon and

230 methylated by the thermochemolysis with C_{10}—C_{13} absent, C_{14}—C_{16} present, but no longer chains. The absence of the ubiquitous C_{18} n-alkanoic methyl ester indicates that these longer C_{14}—C_{16} chains are not simply contamination but that also these were associated to the cysts themselves. The shorter C_3—C_9 n-alkenoic methyl esters are accompanied by (C_4 — C_9) alkanedioic dimethyl esters with a strong dominance of the C_4 representative and, again, provide evidence for a cyst wall with short-chain ester-cross-linked moieties. Fresh *L. polyedrum* cysts do not show any aliphatic signature so that we

235 attribute its presence in the *T. pelagica* cyst wall to diagenetic modification of the initial macromolecule.

The thermochemolysis of cultured *L. polyedrum* cysts (Fig. 7) produced a series of mono- to penta-methoxy-benzenes, providing evidence for carbohydrate hydroxy groups in the cyst-wall polymer (Versteegh et al., 2012). The near absence of such products for the cysts from the Kerguelen Plateau suggests that this signature has been almost completely erased by diagenesis.

240 The detection of benzenes with up to nine attached carbon atoms and phenols with up to four attached carbon atoms fully agrees with the observed chain length distribution of the aliphatic component and again suggests a macromolecule with carbon chains < C_9 chains. These series are longer than for the cultured *L. polyedrum* cysts but shorter than for the *T. pelagica* cysts from the Rhine Graben.

The stronger diagenetic alteration and sulphurisation of the material from the Rhine Graben is also reflected by the relatively

245 higher abundance of masses characteristic for sulphur (*m/z* 64, S2) and alkylthiophenes (*m/z* 97, 111, 125 and 139) whereas oxygen containing moieties are more abundant in the material from the Kerguelen Plateau (*m/z* 93, 107, 121, 135 from Phenols and *m/z* 95, 145 from (benzo)furans) as are alkylbenzenes (*m/z* 79, 105, 119, 133) (Fig. 8). Comparison to mass distributions of pyrolysates of other macromolecules (Fig. 6) demonstrates the much lower aliphatic contribution of the Kerguelen material.

4 Conclusions

250

By analysing remains of the same organism (*T. pelagia*) from two contrasting environmental settings, differences in the composition of the starting materials on the diagenetic process can be excluded. As such, all chemical differences between the cysts from the different depositional settings can be assigned to post-mortem modification of the original biomacromolecule.

255 Specifically, we analysed the composition and structure of *T. pelagica* cysts from the Kerguelen Plateau. Comparison to recent cysts of gonyaulacoid dinoflagellates, the group of which *Thalassiphora* is a member, shows that the fossil cysts to a large extent have been structurally preserved. Diagenetic modification is mainly confined to an increase in C=O and a loss of C-O. Thermochemolysis shows a strong decrease in the production of methoxy benzenes indicating that the initially present hydroxy moieties associated to carbohydrates have become lost diagenetically. The presence of carbon chains up to C_{11} is 260 also attributed to diagenesis since such an aliphatic component is absent in culture-derived gonyaulacoid cysts.

The *T. pelagica* cysts from the Kerguelen Plateau are compositionally very different from coeval specimens from Rhine Graben, despite representing the same species and the absence of any visual indication for these differences upon microscopic examination. These cysts from the Rhine Graben also deviate much more from the modern gonyaulacoid cysts than the specimens from the Kerguelen Plateau. We attribute this to a much stronger diagenetic overprint enforced by the 265 sulphidic diagenetic setting the material from the Rhine Graben has been subject to. This study nicely demonstrates the advantage of using organic particles of narrowly defined (species level) biological sources for unravelling post-mortem modification of organic matter. Furthermore, it leads to the counterintuitive conclusion that the best preservation of molecular structure may not be found where most organic matter is preserved.

5 Code and Data Availability

270

Data are available at https://doi.pangaea.de/10.1594/PANGAEA.905696

6 Author Contributions

Gerard J. M. Versteegh collected the geochemical data interpreted them and wrote the manuscript. Alexander J. P. Houben provided the material and did the palynology. Karin A. F. Zonneveld was responsible for project funding and administration 275 and together with GJMV formulated the overarching research goals and aims. All authors discussed data and earlier manuscript versions.

7 Competing Interests

The authors declare they have no competing interests

280 **8 Acknowledgments**

We thank Henk Brinkhuis (Utrecht University, Royal NIOZ) for his constructive comments on the manuscript. We also thank reviewers N.N and N.N. for their constructive comments, which significantly improved the manuscript. This work has benefited from funding by the German Science Foundation (DFG) Grant MER/MET: 17-87. IODP is thanked for providing the sample utilized in this study.

285 **References**

Allard, B., Templier, J.: Comparison of neutral lipid profile of various trilaminar outer cell wall (TLS)-containing microalgae with emphasis on algaenan occurrence, Phytochem., 54, 369-380, doi: 10.1016/S0031-9422(00)00135-7, 2000.

Allard, B., Templier, J.: High molecular weight lipids from the trilaminar outer wall (TLS)-containing microalgae *Chlorella emersonii, Scenedesmus communis* and *Tetraedron minimum*, Phytochem., 57, 459-467, doi: 10.1016/S0031-9422(01)00071-1, 2001.

Bianchi, T. S., Schreiner, K. M., Smith, R. W., Burdige, D. J., Woodart, S., Conley, D. J.: Redox Effects on Organic Matter Storage in Coastal Sediments During the Holocene: A Biomarker/Proxy Perspective, Ann. Rev. Earth Planet. Sci., 44, 295-319, doi:10.1146/annurev-earth-060614-105417, 2016.

Blokker, P., Schouten, S., van den Ende, H., de Leeuw, J. W., Hatcher, P. G., Sinninghe Damsté, J. S.: Chemical structure of algaenans from the fresh water algae *Tetraedron minimum, Scenedesmus communis* and *Pediastrum boryanum*, Org. Geochem., 29, 1453-1468, doi: 10.1016/S0146-6380(98)00111-9, 1998.

Blom, A. V.: Quelques remarques sur le mécanisme de séchage des peintures à l'huile, Peintures, Pigments, Vernis, 13, 156-162, 1936.

Bogus, K., Harding, I. C., King, A., Charles, A. A., Zonneveld, K. A. F., Versteegh, G. J. M.: The composition and diversity of dinosporin in species of the *Apectodinium* complex (Dinoflagellata), Rev. Palaeobot. Palynol., 183, 21-31, doi:10.1016/j.revpalbo.2012.07.001, 2012.

Bogus, K., Mertens, K. N., Lauwaert, J., Harding, I. C., Vrielinck, H., Zonneveld, K. A. F., Versteegh, G. J. M.: Differences in the chemical composition of organic-walled dinoflagellate resting cysts from phototrophic and heterotrophic dinoflagellates, J. Phycol., 50, 254-266, doi:10.1111/jpy.12170, 2014.

305 Colthup, N. B., Daly, L. H., Wiberly, S. E.: Introduction to Infrared and Raman Spectroscopy, Academic Press Limited, London, 1990.

Durand, B.: Sedimentary organic matter and kerogen. Definition and quantitative importance of kerogen., in: Durand B., Kerogen : Insoluble Organic Matter from Sedimentary Rocks, Editions Technip, Paris, pp. 13-34, 1980.

Ellegaard, M., Figueroa, R., Versteegh, G. J. M.: Dinoflagellate life cycles and diversity: key foci for future research., in:

310   Lewis J. M., Marret F., Bradley L. (eds.), Biological and Geological Perspectives of Dinoflagellates, Geol. Soc. London, pp. 241-54, doi:10.1144/TMS5.24 2013.

Gatellier, J. P. L. A., de Leeuw, J. W., Sinninghe Damsté, J. S., Derenne, S., Largeau, C., Metzger, P.: A comparative study of macromolecular substances of a Coorongite and cell walls of the extant alga *Botryococcus braunii*, Geochim. Cosmochim. Acta, 57, 2053-2068, doi: 10.1016/0016-7037(93)90093-C, 1993.

315   Goth, K., de Leeuw, J. W., Püttmann, W., Tegelaar, E. W.: Origin of Messel Oil Shale kerogen, Nature., 336, 759-761, doi: 10.1038/336759a0, 1988.

Gupta, N. S., Briggs, D. E. G., Collinson, M. E., Evershed, R. P., Michels, R., Pancost, R. D.: Molecular preservation of plant and insect cuticles from the Oligocene Enspel Formation, Germany: Evidence against derivation of aliphatic polymer from sediment, Org. Geochem., 38, 404-418, doi: 10.1016/j.orggeochem.2006.06.012, 2007.

320   Gurdebeke, P. R., Mertens, K. N., Bogus, K., Marret, F., Chomérat, N., Vrielinck, H., Louwye, S.: Taxonomic re-investigation and geochemical characterization of Reid's (1974) species of Spiniferites from holotype and topotype material, Palynol., doi:10.1080/01916122.2018.1465735, 2018.

Harvey, G. R., Boran, D. A., Chesal, L. A., Tokar, J. M.: The structure of marine fulvic and humic acid, Mar. Chem., 12, 119-132, doi: 10.1016/0304-4203(83)90075-0, 1983.

325   Kohnen, M. E. L., Sinninghe Damsté, J. S., ten Haven, H. L., de Leeuw, J. W.: Early incorporation of polysulfides in sedimentary organic matter, Nature, 341, 640-641, doi: 10.1038/341640a0, 1989.

de Leeuw, J. W., Largeau, C.: A review of macromolecular compounds that comprise living organisms and their role in kerogen, coal and petroleum formation, in: Engel M. H., Macko S. A. (eds.), Organic Geochemistry. Principles and Applications, Plenum Press, New York, pp. 23-72, doi: 10.1007/978-1-4615-2890-6_2, 1993.

330   de Leeuw, J. W., Versteegh, G. J. M., van Bergen, P. F.: Biomacromolecules of plants and algae and their fossil analogues, Plant Ecol., 189, 209-233, doi: 10.1007/s11258-005-9027-x, 2006.

Lin, R., Ritz, G. P.: Reflectance FT-IR microspectroscopy of fossil algae contained in organic-rich shales, Appl. Spectroscopy, 47, 265-271, doi:10.1366/0003702934066794, 1993.

Luo, Z., Lim, Z. F., Mertens, K. N., Gurdebeke, P., Bogus, K., Carbonell-Moore, M. C., Vrielinck, H., Leaw, C. P., Lim, P.

335   T., Chomérat, N., Li, X., Gu, H.: Morpho-molecular diversity and phylogeny of *Bysmatrum* (Dinophyceae) from the South China Sea and France, European. J. Phycol., doi:10.1080/09670262.2018.1449014, 2018.

McMurry, H. L., Thornton, V.: Correlation of Infrared Spectra, Anal. Chem., 24, 318-334, doi:10.1021/ac60062a018, 1952.

Mertens, K. N., Gu, H., Takano, Y., Price, A. M., Pospelova, V., Bogus, K., Versteegh, G. J. M., Marret, F., Turner, R. E., Rabalais, N. N., Matsuoka, K.: The cyst-theca relation of *Trinovantedinium pallidifulvum*, with erection of *Protoperidinium*

340 *lousianensis* sp. nov. and their phylogenetic position within the *Conica* group, Palynol., 41, 183-202, doi:10.1080/01916122.2016.1147219, 2016 .

Mertens, K. N., Takano, Y., Yamaguchi, A., Gu, H., Bogus, K., Kremp, A., Bagheri, S., Matishov, G., Matsuoka, K.: The molecular characterization of the enigmatic dinoflagellate *Kolkwitziella acuta* reveals an affinity to the *Excentrica* section of the genus *Protoperidinium*, Syst. Biodiv., doi:10.1080/14772000.2015.1078855, 2015.

345 Mertens, K. N., Wolny, J., Carbonell-Moore, C., Bogus, K., Ellegaard, M., Limoges, A., de Vernal, A., Gurdebeke, P., Omura, T., Al-Muftah, A., Marsuoka, K.: Taxonomic re-examination of the toxic armored dinoflagellate *Pyrodinium bahamense* Plate 1906: Can morphology or LSU sequencing separate *P. bahamense* var. *compressum* from var. *bahamense*? Harmful Algae, 41, 1-24, doi:10.1016/j.hal.2014.09.010, 2015.

Nissenbaum, A., Kaplan, I. R.: Chemical and isotopic evidence for the in situ origin of marine humic substances, Limnol.
350 Oceanogr., 17, 570-582, doi:10.4319/lo.1972.17.4.0570, 1972.

Nunn, S., Nishikida, K.: Advanced ATR correction algorithm, Thermo Fisher Appl. Notes., Note 50581, 1-3, 2008.

Rontani, J. F.: Photooxidative and autoxidative degradation of lipid components during the senescence of phototrophic organisms, in: , Phytochemistry Research Progress, Nova Science Publishers, Hauppauge, NY, pp. 115-44, 2008.

Stankiewicz, B. A., Briggs, D. E. G., Michels, R., Collinson, M. E., Flannery, M. B., Evershed, R. P.: Alternative origin of
355 aliphatic polymer kerogen, Geol., 28, 559-562, doi:10.1130/0091-7613(2000)28<559:AOOAPI>2.0.CO;2, 2000.

Stankiewicz, B. A., Scott, A. C., Collinson, M. E., Finch, P., Mösle, B., Briggs, D. E. G., Evershed, R. P.: Molecular taphonomy of arthropod and plant cuticles from the Carboniferous of North America: implications for the origin of kerogen, J. Geol. Soc. London, 155, 453-462, doi: 10.1144/gsjgs.155.3.0453, 1998.

Vandenbroucke, M., Largeau, C.: Kerogen origin, evolution and structure, Org. Geochem., 38, 719-833, doi:
360 10.1016/j.orggeochem.2007.01.001, 2007.

Versteegh, G. J. M., Blokker, P., Bogus, K., Harding, I., Lewis, J., Oltmanns, S., Rochon, A., Zonneveld, K. A. F.: Infra red spectroscopy, flash pyrolysis, thermally assisted hydrolysis and methylation (THM) in the presence of tetramethylammonium hydroxide (TMAH) of cultured and sediment-derived *Lingulodinium polyedrum* (Dinoflagellata) cyst walls, Org. Geochem., 43, 92-102, doi:10.1016/j.orggeochem.2011.10.007, 2012.

365 Versteegh, G. J. M., Blokker, P., Marshall, C. R., Pross, J.: Macromolecular composition of the dinoflagellate cyst *Thalassiphora pelagica* (Oligocene, SW Germany), Org. Geochem., 38, 1643-1656, doi: 10.1016/j.orggeochem.2007.06.007, 2007.

Versteegh, G. J. M., Blokker, P., Wood, G., Collinson, M. E., Sinninghe Damsté, J. S., de Leeuw, J. W.: An example of oxidative polymerization of unsaturated fatty acids as a preservation pathway for microalgal organic matter, Org. Geochem.,
370 35, 1129-1139, doi: 10.1016/j.orggeochem.2004.06.012, 2004.

Wojdyr, M.: Fityk: a general-purpose peak fitting program, J. Appl. Crystallogr., 43, 1126-1128, doi: 10.1107/S0021889810030499, 2010.

375

Table 1. Compounds identified in the pyrolysate[a]

#	Name	M+
1	Methylcyclopentadiene (C_6H_8)	80
2	Benzene	78
3	Cyclohexadiene	80
4	2,5 Dimethylfuran	96
5	Toluene	92
6	? C_8H_{12}	108
7	Cyclopentenone + Furfural	96 + 82
8	Ethyl-benzene	106
9	2-Propylfuran	110
10	1,3 + 1,4 dimethylbenzene	106
11	Pentanoic acid	102
12	1,2 dimethylbenzene	106
13	Styrene	104
14	2-Methyl-2-cyclopentenone (67, 96)	67, 96
15	Acetylfuran	95, 110
16	Cyclopentandione	69, 98
17	Cyclohexenone	68, 96
18	Propylbenzene	120
19	3-Methyl-2-cyclopentenone	96
20	3-Methylbenzene + Unknown (43/85)	120
21	Phenol	94
22	$C_{3:1}$ Benzene + 3-Methylbenzene	118, 120
23	Cyclohexandione (70,112)	70, 112
24	Octanal	128
25	Methylcyclopentandione (69,112)	112
26	Limonene (?)	136
27	Indane	118
28	2,3-Methylcyclopentenone (67,110)	110
29	Indene	116
30	Methyl-propylbenzene	134
31	Methylphenol	108
32	C_4 Benzene	134

Table 1. Compounds identified in the pyrolysate[a]

33	C_3 Cyclopentenone ? (109,124)	124
34	Acetophenone	120
35	Methylbenzaldehyde	120
36	Methylbenzaldehyde	120
37	$C_{3:1}$ Benzene + C_3 Benzene	132 + 134
38	4-Ethenyl, C_2-benzene	132
39	Nonenol (no 114)	142
40	C2 Phenol	122
41	1-Acetylcyclohexene + C_1-Benzofuran	124 + 132
42	3-ethyl-2-hydroxy-2-cyclopentenone	126
43	Methylindene	130
44	C_5 Benzene	146
45	Naphthalene	128
46	Trimethylphenol (121, 136)	136
47	C_2 Benzofuran	146
48	C_2-Indene	144
48	Indanone	132
49	Methylnaphthalene	142
50	Naphthalenone	146
51	Me-Indanone	146
52	C_2-Indanone	160
53	1,3 Diphenylpropane	196

[a]Peak numbers refer to Fig. 5

380

385

390

395

Table 2. Compounds identified in the thermochemolysate[a]

#	Name	M+
1	Trimethylamine - TMAH product	59
2	Cyclopentadiene	66
3	$C_{3:1}$ Fatty acid - Me	86
4	Cyclohexadiene	80
5	Benzene	78
6	Methyl-cyclohexadiene	94
7	Dimethylamino-acetonitrile - TMAH product	84
8	Toluene	92
9	Ethylbenzene	106
10	1,3 + 1,4 Dimethylbenzene	106
11	Styrene + 1,2 Dimethylbenzene	104 + 106
12	2-Methyl-2-cyclopenten-1-one	96
13	Isopropylbenzene	120
14	Propenylbenzene	120
15	Propylbenzene	120
16	1-Methyl-3-ethylbenzene	120
17	1-Methy-4-ethylbenzene	120
18	1,3,5-Trimethylbenzene	120
19	Methylstyrene + 1-Methyl-2-ethylbenzene	118 + 120
20	Methylstyrene	118
21	Indane	118
22	Methoxyphenol	108
23	Indene	116
24	C_4 Benzene	134
25	Acetophenone	120
26	C_4 Benzene	134
27	$C_{4:1}$ Benzene	132
28	Dimethoxybenzene (123, 138)	138

Table 2. Compounds identified in the thermochemolysate[a]

29	C_1 Indene	130
30	Naphthalene	128
31	Methylbenzoicacid	150
32	C_2 Indene	144
33	Indanone	132
34	Methylnaphthalene	142
35	Methoxybenzoicacid - Me	166
36	Trimethoxybenzene	168
37	C_3 Indene	158
38	Diaromatic $C_{12}H_{10}$	154
39	Ethylnaphthalene	156
40	C_2 Naphthalene	156
41	$C_{2:1}$ Naphthalene	154
42	Acenaphthylene	152
43	Dibenzoicacid-Me	194
44	C_3 Naphthalene	170
45	Methyl diaromatic	168
46	Dimethoxybenzoicacid-Me	196
47	Diaromatic $C_{13}H_{10}$ (e.g. Fluorene)	166
48	Triaromatic $C_{14}H_{10}$	178

[a]Peak numbers refer to Fig. 7.

400
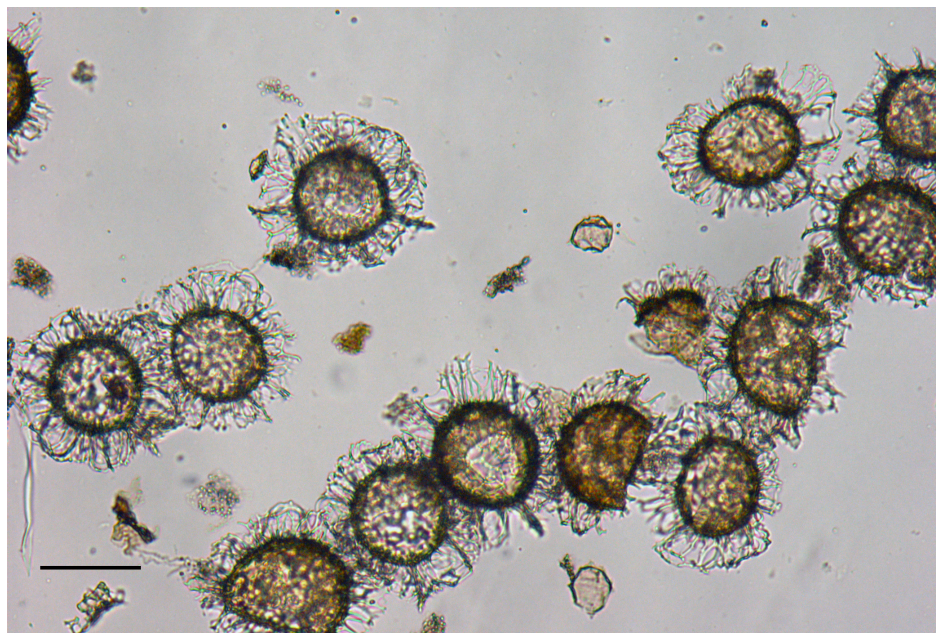
Figure 1: **Microphotograph of the *Thalassiphora pelagica* assemblage from the Kerguelen Plateau prior to purification with a sieve with 50 µm pore size. Scale bar = 100 µm.**

405

410
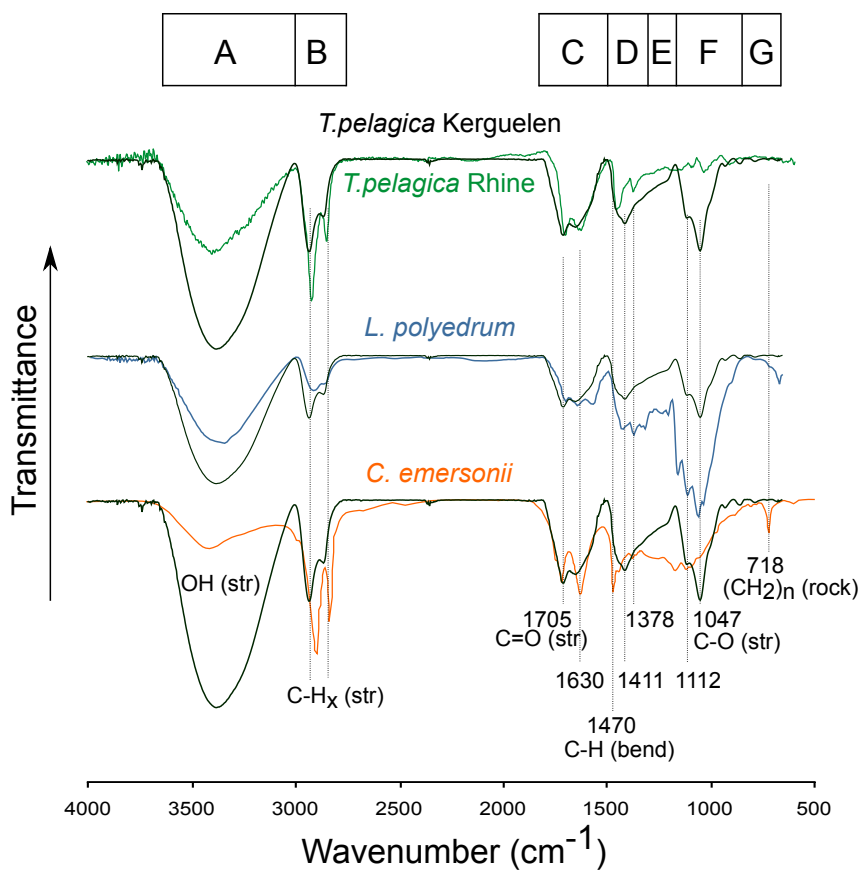
415   Figure 2: **Fourier transform infra red spectra of algae, *Thalassiphora pelagica* from the Kerguelen Plateau in black compared to:**
A *Thalassiphora pelagica* from the Rhine Graben (green line) (Versteegh et al., 2007); B. *Lingulodinium polyedrum* cysts from
culture (blue line) (from Versteegh et al., 2012); C. *Clorella emersonii* (orange line) (adapted from Allard, and Templier, 2000).
Capotal A-G refer to spectral regions discussed in the text. Numbers refer to wavenumbers in cm^{-1}.

420
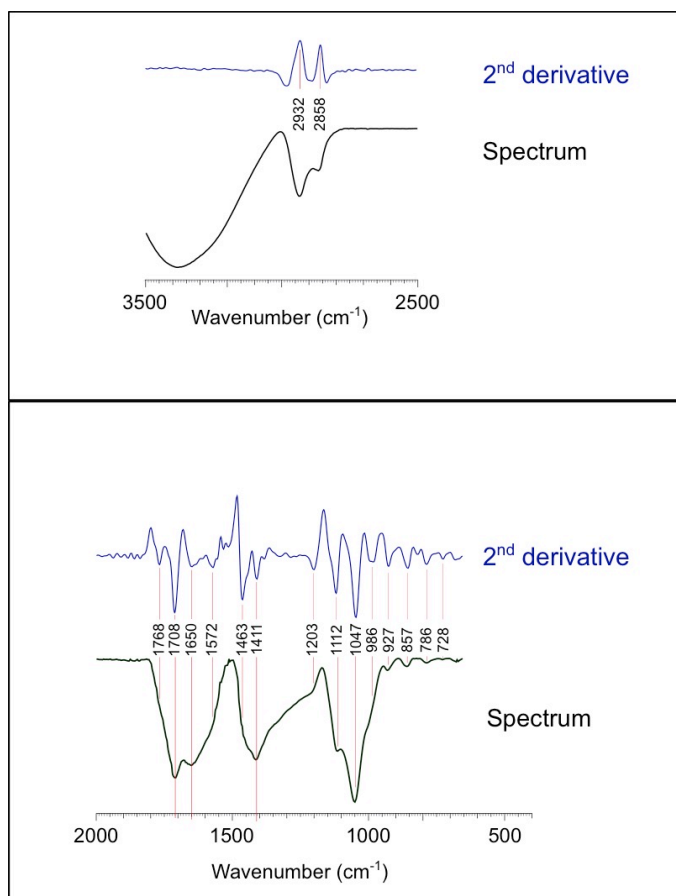
Figure 3: **Detailed views of the fourier transform infra red spectrum of *Thalassiphora pelagica* from the Kerguelen Plateau with**
425   **second derivative. Top Panel, detail of the 3500-2500 cm^{-1} region of the FTIR absorption spectrum (transmission mode) of *T.***
pelagica*. Lower panel, detail of the 2000—700 cm^{-1} region with the maxima of the spectrum 2nd derivative showing the locations
of absorption bands.

430
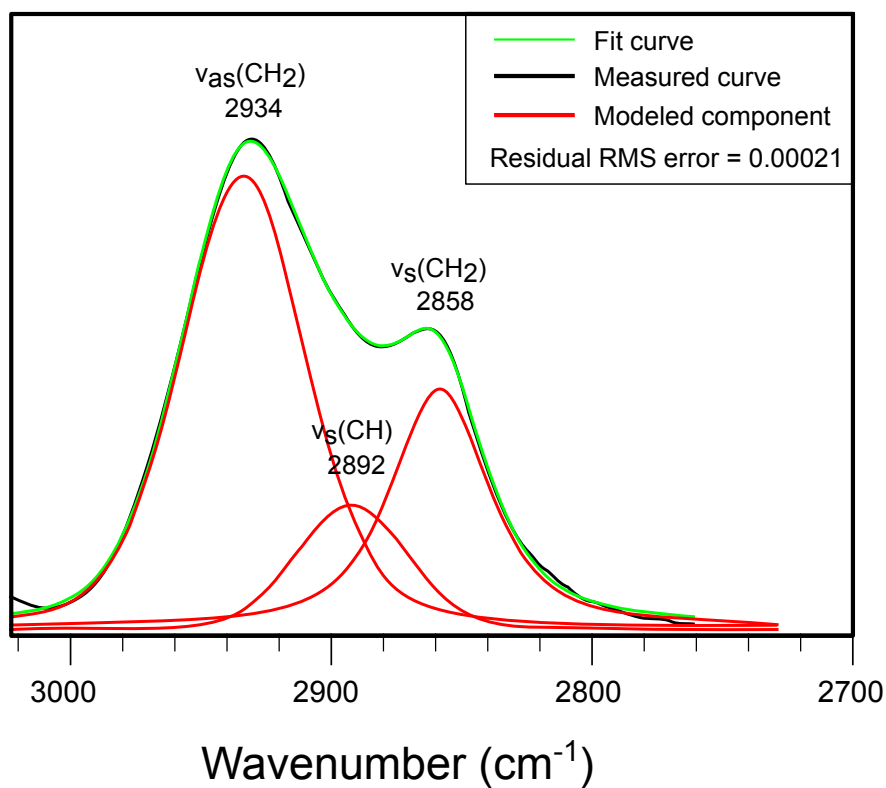
Figure 4: **Deconvolution of the CH$_x$ absorption bands for the 3100-25700 cm^{-1} region demonstrating the absence of significant CH$_3$ absorption. Modelled curves are a mixed Lorenzian and Gaussian (L+G) or Gaussian only (G). Percentages indicate the proportion to which the curve represents the Lorentzian function. The curve at 2934 cm^{-1} is 25% Lorentzian, intensity 2.4 and** 435 **width 57.; the curve at 2829 cm^{-1} is purely Gaussian with intensity 0.6 and width 51; the curve at 2858 cm^{-1} is 70% Lorenzian with intensity 1.3 and width 45.**
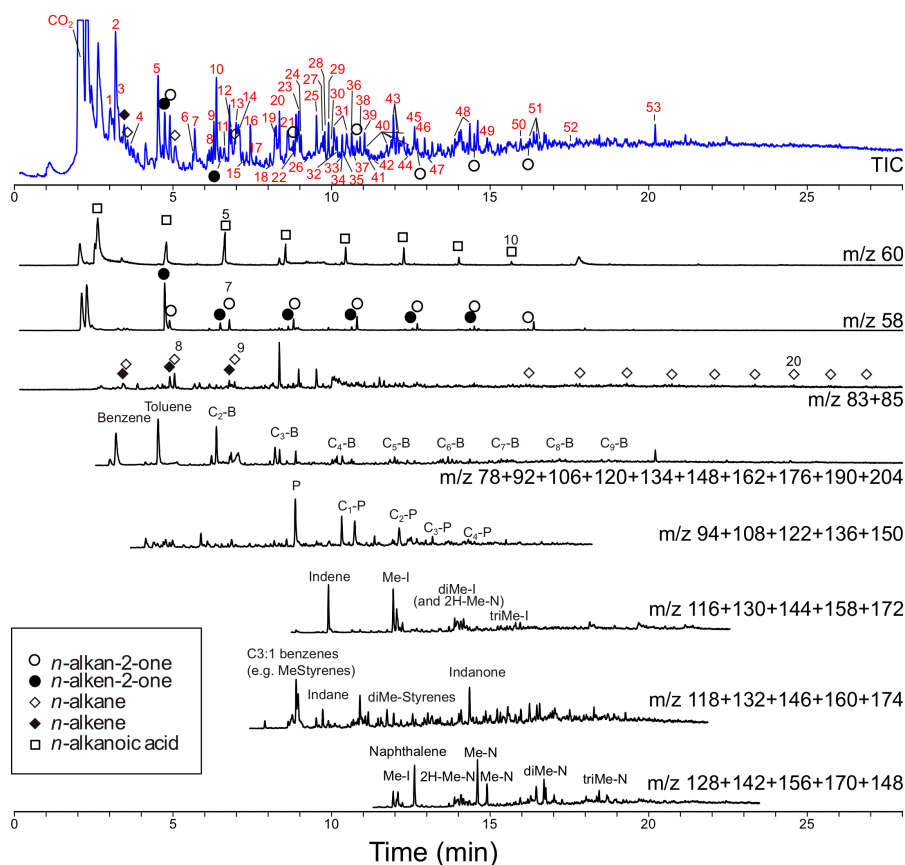
Figure 5: **Chromatogram and mass chromatograms of pyrolysed *Thalassiphora pelagica* cysts from the Kerguelen Plateau. For the total ion current (TIC) the compound names corresponding to numbered peaks (red numbers) are given in Table 1. For the mass chromatograms B=benzene, P=Phenol, N= Naphthalene, I= Indene, 'C-with-number' indicates the number of carbon atoms added to the basic structure.**
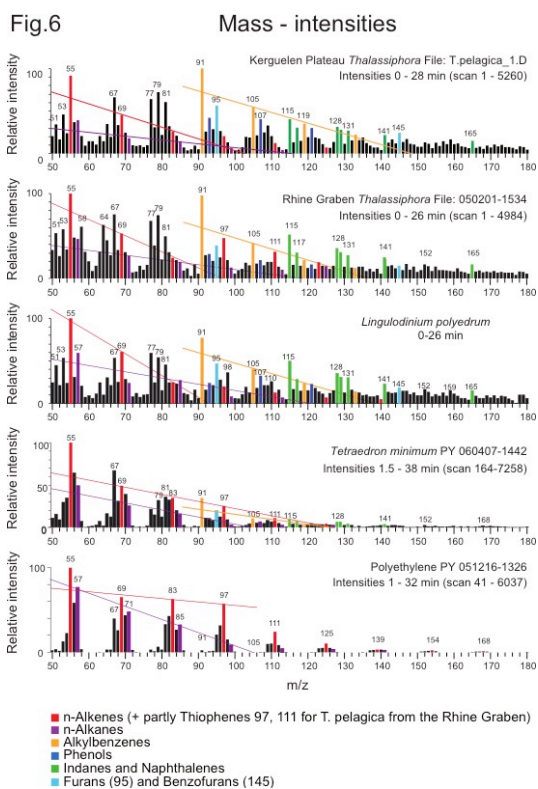
450 Figure 6: **Mass intensity plots of the total chromatograms of (a)** *Thalassiphora pelagica* **from the Kerguelen Plateau, (b)**
     Thalassiphora pelagica **from the Rhine Graben (Versteegh et al., 2007), (c) Recent** *Lingulodinium polyedrum* **(Versteegh et al.,**
     2012), (d) *Tetraedron minimum* **and (e) polyethene. The lines connect masses indicative for** *n*-alkenes (*m/z* **69, 83, 97),** *n*-alkanes (
     m/z **57, 71, 85, 99) and alkylbenzenes (***m/z* **105, 119) , respectively. Note that the total ion current of polyethene is dominated by**
     series of ions meeting the criteria C_nH_{2n-1} **and** C_nH_{2n+1}, **reflecting the highly aliphatic nature of the macromolecule. Note for** *T.*
455 *pelagica* **the relatively high aromatic contribution (orange bars; m/z 91, 105, 115, 117, 128, 129, 131) in comparison to the**
     'aliphatic-derived' fragments of alkanes and alkenes, and for *T. pelagica* **from the Rhine Graben the high relative contribution of**
     m/z 97 and 111 as compared to m/z 69 and 83 which is attributed to the presence of alkylthiophenes.
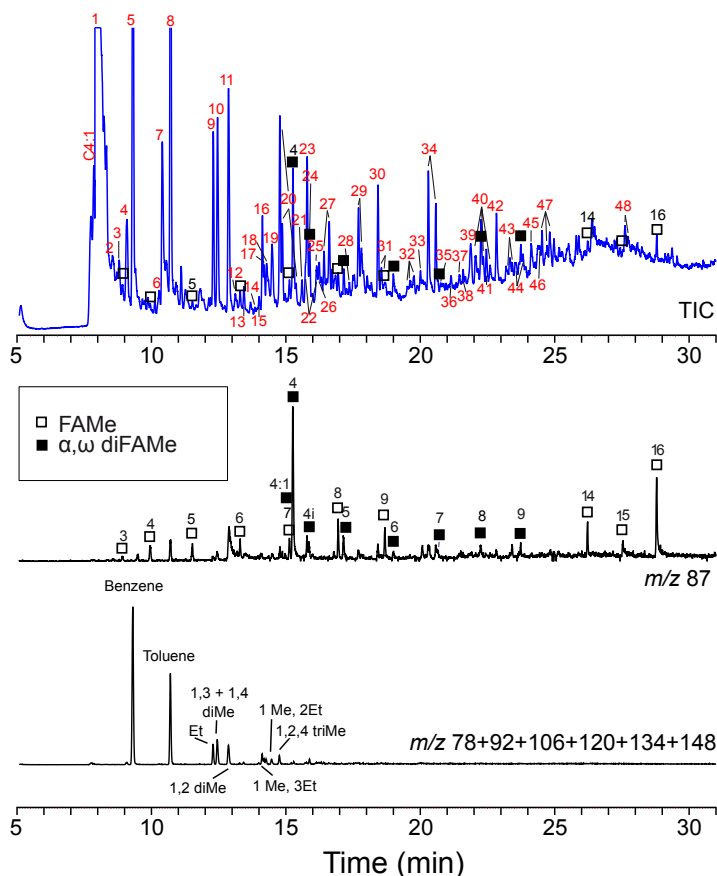
Figure 7: **Chromatogram and mass chromatograms of *Thalassiphora pelagica* cysts from the Kerguelen Plateau after THM-GC-MS. Open squares *n*-alkanoic acids; closed squares *n*-alkanedioic acids. Black numbers indicate the number of carbon atoms of the compound. Red numbers refer to compound names listed in Table 2. Upper panel total ion current (TIC).; Lower panel mass chromatogram of m/z = 87 showing methyl esters of *n*-alkanoic acids and *n*-alkanedioic acids; 4:1 refers to the butenedioic acid, 4i refers to the iso-butanedioic acid. FAMe stands for fatty acid methyl ester.**
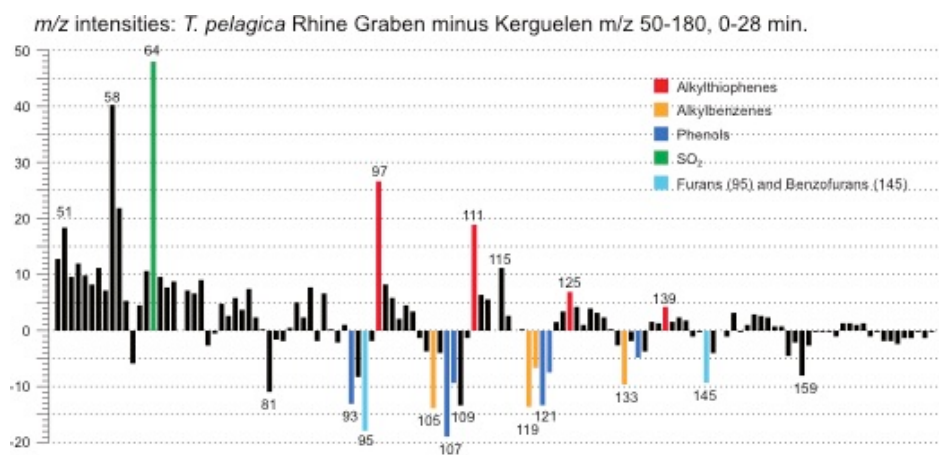
NB: possible *m/z* 58 fragments: C_3H_6O, C_4H_{10}, C_2S

Figure 8: **Relative mass intensities of the total chromatograms of *Thalassiphora pelagica* from the Rhine Graben minus those of *Thalassiphora pelagica* from the Kerguelen Plateau (Versteegh et al., 2007). Masses with abundances < 0 are more abundant in the specimens from the Kerguelen Plateau. Note the masses indicating sulphur containing fragments (thiophenes) are more important in the specimens from the Rhine Graben whereas masses characterizing oxygen containing fragments (furans, phenols) and alkylbenzenes are more abundant in specimens from the Kerguelen Plateau.**

470